



Integrated soluble polymer and mesoporous silica as a double-type support to immobilize tertiary amine–Ru/diamine–bifunctionality for aza–addition/reduction cascade reaction



Ming Gao, Fengwei Chang, Shitong Wang, Zeyang Liu, Zhitong Zhao, Guohua Liu*

Key Laboratory of Resource Chemistry of Ministry of Education, Shanghai Key Laboratory of Rare Earth Functional Materials, Shanghai Normal University, Shanghai 200234, PR China

ARTICLE INFO

Article history:

Received 3 May 2019

Revised 24 June 2019

Accepted 1 July 2019

Keywords:

Heterogeneous catalysis

Supported catalysts

Asymmetric transfer hydrogenation

Michael addition

Immobilization

Mesoporous materials

ABSTRACT

Exploiting advantages of a double-type support to create an active site–isolated heterobifunctional catalyst is beneficial to an efficiently sequential organic transformation. Herein, an integrated soluble polymer and mesoporous silica as a double-type support to immobilize the tertiary amine–Ru/diamine–bifunctionality for the construction of an active site–isolated catalyst is developed, where the tertiary amine–functionality is tethered in the outer soluble polymer and chiral ruthenium/diamine–functionality is anchored within the inner mesoporous silica. Electron microscopy images, together with analyses of solid–state NMR spectra, disclose that catalyst possesses the uniformly distributive morphology with well–defined single–site ruthenium/diamine active centers. As envisaged, the heterobifunctional catalyst performs a highly efficient aza–Michael addition/asymmetric transfer hydrogenation enantioselective cascade reaction, where the outer tertiary amine–functionality enables a high reactivity to afford β –secondary amino ketones via an aza–Michael addition reaction of enones and amines, and the inner chiral ruthenium/diamine–functionality guarantees a high enantioselectivity to chiral γ –secondary amino alcohols via an asymmetric transfer hydrogenation of β –secondary amino ketones. Furthermore, this catalyst can also be recovered easily and recycled for six runs, showing a practical preparation of aryl–substituted γ –secondary amino alcohols.

© 2019 Elsevier Inc. All rights reserved.

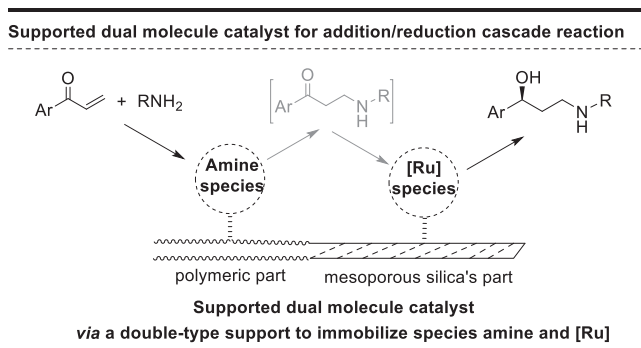
1. Introduction

Development of supported dual molecule catalysts for multi–step sequential enantioselective reactions has been attracting extensive interest, where some reviews are well–documented recently [1–4]. So far, the common strategy for immobilization of dual functionality is through single–type supports, where numerous supported bifunctional catalysts have successfully applied to various cascade reactions, especially the use of single–type mesoporous silica–supported [5–11] and soluble polymer–supported chiral bifunctional catalysts [12–14]. Outstanding feature of silica–supported bifunctional catalysts is their orderly mesoporous structures with adjustable channels and highly mechanical stabilities, and some designed and explored synergistic effects enhance reactivity and enantioselectivity [7,8]. Prominent contributions of soluble polymer–supported bifunctional catalysts are attributed to the high–dispersibility in reaction systems because a mimic homo–like catalytic environment benefits the mass transfer to

promote catalytic efficiency [13]. Despite these significant achievements, the only use of mesoporous silica and soluble polymer as single–type supports has still some limitations, especially their applications in multi–step enantioselective organic transformations [15]. A general restriction comes from single–type support itself. Rigid silica–supported catalysts have the diffused shortcoming of mass transfers that lead to the decreased reaction rates, whereas flexible polymer–supported catalysts have the swelling disadvantage of soluble polymers that result in the poor enantioselectivities. A special restriction lies in a strict and subtle demand of chiral catalytic environment in an enantioselective cascade reaction because dual functionality in a single–type support must possess an ability to differentiate two possible enantiomers and more intermediates during a complicated catalysis process. However, due to the drawback of cross interference, dual functionality in a single–type support is quite difficult to work together well. Thus, utilization of a double–type support to immobilize two species has a significant superiority in a multi–step sequential enantioselective organic transformation as shown in Scheme 1, which not only exploits the respective advantages of a double–type support

* Corresponding author.

E–mail address: ghliu@shnu.edu.cn (G. Liu).



Scheme 1. Construction of a supported dual molecule catalyst via a double-type support for the aza-Michael addition/reduction cascade reaction.

and complements the drawbacks of a single-type support but also benefits to create site-isolation-featured catalysts.

Chiral γ -secondary amino alcohols and analogues are important pharmaceutical intermediates for the synthesis of the highly value-added antidepressants [16–21]. General preparations of chiral γ -secondary amino alcohols is through a single-step asymmetric hydrogenation of prochiral β -amino ketones under homogeneous conditions [22–28], where the main works employ the Rh-bisphosphine-complexes, Rh-Duanphos complex and analogues as chiral catalysts to convert various β -amino ketones into chiral γ -secondary amino alcohols. Recently, we also report an asymmetric transfer hydrogenation (ATH) method to enable the preparation of optically pure γ -secondary amino alcohols [29]. However, due to the problems of environmentally unfriendly solvents, expensive transition-metal recycling and poor catalysis efficiency, their applications are still greatly limited. Therefore, based on the consideration of green catalysis, development of an atom-economic, environmentally friendly cascade process for highly efficient preparation of optically pure γ -secondary amino alcohols is highly desirable.

In this contribution based on our efforts in the cascade reactions [30–32], we integrate the soluble polymer and mesoporous silica as a double-type support to construct a supported dual molecular catalyst (Scheme 1), where the tertiary amine-functionality is tethered in the outer soluble polymer and the chiral ruthenium/diamine-functionality is anchored within the inner mesoporous silica. The advantage of this heterobifunctional catalyst is the catalytically active site-isolated, where the outer tertiary amine-functionality enables a high reactivity in aza-Michael addition reaction due to the highly dispersed benefit of soluble polymer in an aqueous medium whereas the inner chiral ruthenium/diamine-functionality in silica network guarantees high enantioselectivity in asymmetric transfer hydrogenation owing to the maintainable chiral catalytic environment. As we envisaged, this heterobifunctional performs an efficiently enantioselective cascade reaction in an environmentally friendly medium, affording chiral aryl-substituted γ -secondary amino alcohols with high yields and enantioselectivities.

2. Experimental

2.1. Preparation of catalyst **5**

In a typical synthesis, (*The first step for the synthesis of 2*) 0.25 g (0.17 mmol) of cetyltrimethylammonium bromide (CTAB) was added to an aqueous solution (120 mL) of NaOH (0.88 mL, 2.0 M) at 70 °C. After the dissolution of CTAB, 2.0 g of (9.62 mmol) of tetraethoxysilane (TEOS) was added, and the mixture was stirred for 5–10 min. After that, 0.10 g (0.20 mmol) of ArDPEN-siloxane (**1**) was added to the system by dropwise, the mixture was stirred for another 5–10 min. Finally, the mixture was stirred vigorously

for two hours at 80 °C. After cooling to room temperature, the solids were collected by centrifugation and washed repeatedly with excess distilled water. The collected solids (1.36 g) were suspended in 20.0 mL of dry toluene and 0.45 g (2.14 mmol) of triethoxy(vinyl)silane in 2 mL of dry toluene was added, and the mixture was stirred overnight at ambient temperature. The surfactant template was removed by refluxing in a solution (80.0 mg of ammonium nitrate in 120 mL of ethanol) at 60 °C for 12 h. The solids were filtered and washed with excess ethanol, and dried at ambient temperature under vacuum overnight to afford Vinyl@ArDPEN@MSN (**2**) (1.52 g) as a white powder. (*The second step for the synthesis of 4*) 1.0 g of **2**, 0.25 g (2.95 mmol) of *N,N*-dimethyl prop-2-en-1 were weighed into a 100 mL nitrogen flask and dissolved in 20 mL of distilled DMSO. Then, 65.5 mg (2% mol) of 2,2-azobisisobutyronitrile (AIBN) was added at room temperature. After a degassed period by three freeze-pump-thaw cycles, the flask was placed into the oil to polymerize at 60 °C for 6.0 h. After cooling to room temperature, the solids were filtered and washed with excess ethanol, and dried at ambient temperature under vacuum overnight to afford P@ArDPEN@MSN (**4**) as a white powder (0.11 g). (*The third step for the synthesis of 5*) The collected solids (0.50 g) was suspended in 20.0 mL of dry CH₂Cl₂, 50.0 mg of (MesRuCl₂)₂ (0.086 mmol) was added at room temperature, and the resulting mixture was stirred at 25 °C for 12 h. The mixture was filtered and rinsed with excess CH₂Cl₂. After Soxhlet extraction for 4 h in CH₂Cl₂, the solid was dried at ambient temperature under vacuum overnight to afford P@MesRuArDPEN@MSN (**5**) (0.51 g) light-red powder. TG analysis showed that the tertiary amine-loadings were 1.02% (1.6414 mg, 0.1172 mmol of N-loadings per gram of catalyst), and Ru-loadings were 1.81% (11.8610 mg, 0.1164 mmol of the Ru-loadings per gram of catalyst) that was consistent with the Ru loadings (11.9103 mg, 0.1167 mmol) per gram of catalyst detected by an inductively coupled plasma optical emission spectrometer (ICP-OES) analysis. ¹³C CP/MAS NMR (161.9 MHz): 157.8–119.1 (C of pH and Ar groups), 106.8, 103.3 (C of mesitylene), 78.3–74.6 (CH of -NCHPh), 63.5, 57.3 (C of CH₃N- and -CH₂N-), 39.9–25.6 (-CH₂CH₂-), 21.9 (CH₃ of mesitylene), 17.6 (CH₂ of -CH₂Ar), 12.5 (CH₂ of -CH₂Si) ppm. ²⁹Si MAS/NMR (79.4 MHz): T³ (δ = -58.4 ppm), T³ (δ = -68.9 ppm), Q² (δ = -92.9 ppm), Q³ (δ = -102.8 ppm), Q⁴ (δ = -112.1 ppm).

2.2. General procedure for the cascade reaction

In a typical procedure, catalyst **5** (8.59 mg, 1.0 μ mol of Ru based on ICP analysis, and 1.01 μ mol of N based on TG analysis), enones (0.10 mmol), amines (0.11 mmol), HCOONa (1.0 mmol), and 2.0 mL of ⁱPrOH/H₂O (v/v = 1:1) were added sequentially to a 10.0 mL round-bottom flask. The mixture was then stirred at 40 °C for 2.5–12 h. After completion of the reaction, the catalyst was separated by centrifugation (10,000 rpm) for the recycling experiment. The aqueous solution was extracted with ethyl ether (3 \times 3.0 mL). The combined ethyl ether extracts were washed with aqueous Na₂CO₃ and brine, and dehydrated with Na₂SO₄. After evaporation of ethyl ether, the residue was purified by silica gel flash column chromatography to afford the desired product. The *ee* values were determined by an HPLC analysis using a UV-Vis detector and a Daicel chiralcel column (Φ 0.46 \times 25 cm).

3. Results and discussions

3.1. Synthesis and structural characterization of the heterobifunctional catalyst **5**

A simple three-step procedure for the assembly of the tertiary amine-functionalized polymer onto the MesRuArDPEN-

functionalized mesoporous silicate nanoparticles (MSNs) provided the bifunctional catalyst, abbreviated as P@MesRuArDPEN@MSN (5), (MesRuArDPEN: [33–36] Mes = Mesitylene; 1,3,5-trimethylbenzene and ArDPEN: (*S,S*)-4-((trimethoxysilyl)ethyl)phenylsulfonyl-1,2-diphenylethylene-diamine), as shown in Scheme 2. In the first step, the co-condensation of tetraethoxysilane (TEOS) and (*S,S*)-ArDPEN-siloxane (1) using cetyltrimethylammonium bromide (CTAB) as a template [37,38], followed by the postgrafting of triethoxy(vinyl)silane, led to a vinyl/ArDPEN-functionalized nanoparticles, Vinyl@ArDPEN@MSN (2). Next, the direct complexation of 2 and (MesRuCl₂)₂ gave a parallel catalyst 3, abbreviated as MesRuArDPEN@MSN (3), as a light-red powder. In the second step, the free radical polymerization [39–41] of 2 and *N,N*-dimethyl prop-2-en-1-amine produced P@ArDPEN@MSN (4) as a white powder. In the third step, catalyst 5 as a light-red powder could be steadily obtained by a similar complexation of 4 with (MesRuCl₂)₂ (see SI in Experiments and in Figs. S1 and S2).

Fig. 1 showed the solid-state ¹³C cross-polarization (CP)/magic angle spinning (MAS) NMR spectra of catalyst 5, disclosing its well-defined single-site MesRuArDPEN-functionality within its mesoporous silica network. It was found that catalyst 5 and its parent material 4 presented general carbon signals between $\delta = 70$ and 75 ppm for the carbon atoms of the $-NCHPh$ moiety and between $\delta = 121$ and 168 ppm for the aromatic carbon atoms in the ArDPEN groups, suggesting the successful incorporation of chiral ligand within the silica network. Catalyst 5 exhibited characteristic peaks at 107.7 and 104.2 ppm for the carbon atoms of the aromatic ring, and at 22.5 ppm for the attached methyl carbon atoms in mesitylene, which were absent in the spectrum of 4. This finding demonstrated that catalyst 5 possessed the similar well-defined single-site active centers to its homogeneous MesRuTsDPEN [33] due to their same chemical shift values, which could be further confirmed by the XPS investigations since catalyst 5 and its homogeneous MesRuTsDPEN had the similar Ru 3d^{5/2} electron binding energy (281.68 eV versus 281.62 eV) (see SI in Fig. S3). In addition, the observed peaks denoted by asterisks were attributed to the rotational sidebands that often appeared in the MAS high-speed rotation process. Solid-state ²⁹Si magic angle spinning (MAS) NMR spectra further demonstrated that catalyst 5 was composed of inorganic and organic silica compositions owing to the presence of two groups of typical silica signals (Q-series signals for inorganic silica and T-series signals for organic silica), as shown in Fig. 2. It was found that their chemical shift values were similar to those reported in the literature (T-series: -58.5 and -67.5 ppm for T² of [R(HO)Si(OSi)₂] and T³ of [RSi(OSi)₃]. Q-series: -91.5 , -101.5 , and -110.0 ppm for Q² of [(HO)₂Si(OSi)₂], Q³ of [(HO)Si(OSi)₃], and Q⁴ of [Si(OSi)₄], respectively) [42]. Notably, the contents of inorganic Q-series signals were higher than those

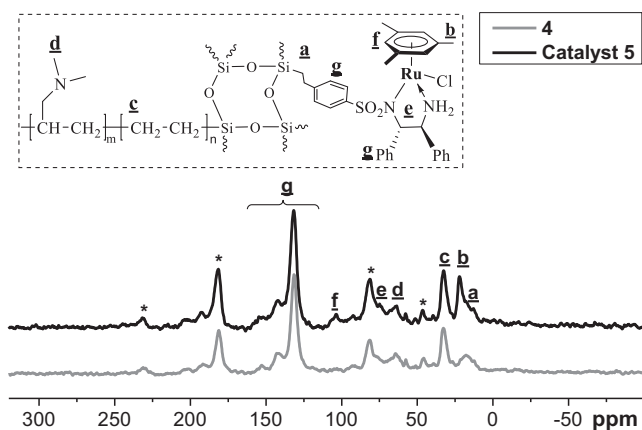


Fig. 1. Solid-state ¹³C CP/MAS NMR spectra of 4 and catalyst 5.

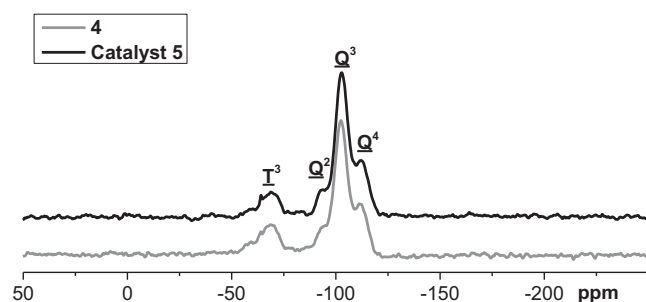


Fig. 2. Solid-state ²⁹Si CP/MAS NMR spectra of 4 and catalyst 5.

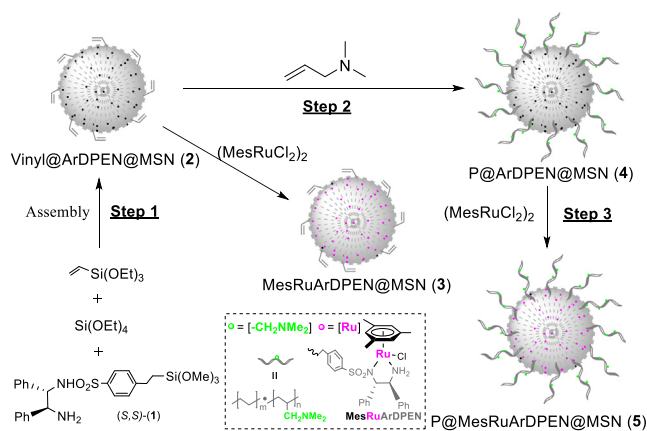
of organic T-series signals, suggesting that catalyst 5 mainly possessed the inorganic silicate R-Si(OSi)₃ species as its main silica network with a small part of organic silicate R-Si(OSi)₃ species (R = alkyl-linked chiral functionalities and polymers) tethered in its silica wall.

The structural morphology from the scanning electron microscopy (SEM) showed that catalyst 5 was uniformly distributed, where the average size of nanoparticles was about 45 nm (Fig. 3a). Furthermore, the transmission electron microscopy (TEM) also disclosed its mesoporous structure (Fig. 3b), which could be confirmed by its nitrogen adsorption-desorption isotherm (Fig. 4) owing to a similar typical IV character with an H₁ hysteresis loop to a pure MSN₅ material [37].

3.2. Catalytic performance of the heterobifunctional catalyst

3.2.1. Catalytic property

With the well-established heterobifunctional catalyst 5 in hand, we chose the cascade reaction of 1-phenylprop-2-enone and aniline as a model reaction to examine its catalytic property in the aza-Michael addition/ATH one-pot cascade process. Owing to the environmentally friendly cosolvent system of water and alcohols could be used in the single-step aza-Michael addition reaction [43] and in the single-step asymmetric transfer hydrogenation [35,44–49], the tested reaction was carried out in the ⁱPrOH/H₂O (1:1, v/v) cosolvent system with 1.0 mol% of ruthenium loadings and 1.02 mol% the tertiary amine loadings in 5 as a catalyst and sodium formate as a hydrogen resource at 40 °C according to the optimal conditions [30]. The result showed that the 5-catalyzed aza-Michael addition/ATH one-pot enantioselective cascade reaction could produce the targeting products of (*S*)-1-phenyl-3-(phenylamino)propanol in 96% yield with 96% ee, which was slightly better than that (95% yield with 95% ee)



Scheme 2. Preparation of the heterobifunctional catalyst 5.

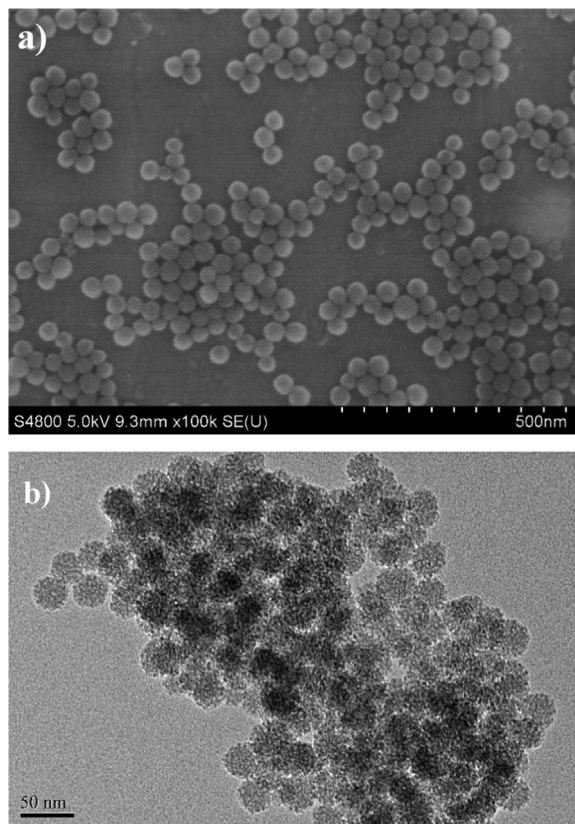


Fig. 3. (a) SEM images of **5**, (b) TEM image of **5**.

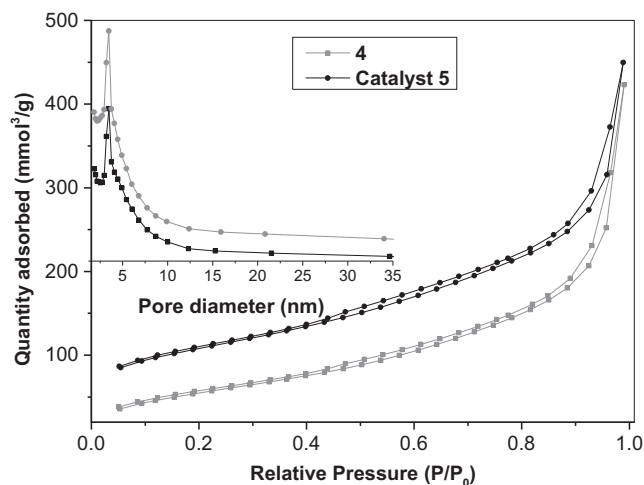


Fig. 4. Nitrogen adsorption–desorption isotherms of **4** and catalyst **5**.

attained with the inorganic Na_2CO_3 as an aza–Michael catalyst and homogeneous MesRuTsDPEN as an ATH catalyst in one-pot cascade reaction under the homogeneous conditions. In particular, such a result was obviously higher than that attained with the physically mixed *N,N*-dimethylprop–2-en–1-amine and the parallel catalyst **3** as dual catalysts (Table 1, entry 1 versus entry 2) because the latter needed 12 h to reach its catalytic completion. This finding revealed the benefit of the outer polymeric parts in the catalyst **5** because of the obviously enhanced reaction rate. It was worth mentioning that this reaction rate in the **5**-catalyzed aza–Michael addition/ATH cascade reaction was nearly five times that in the previously reported yolk–shell-structured heterogeneous catalyst

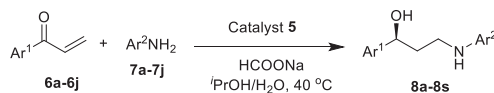
without the polymer-coating layer [30], further confirming the superiority of catalyst **5** equipped with the outer soluble polymer-coating layer. Also, it was found that this result was markedly better than that obtained with the physically mixed *N,N*-dimethylprop–2-en–1-amine and homogeneous MesRuTsDPEN as dual catalysts (Table 1, entry 1 versus entry 3). This observation suggested that the active site–isolation–featured catalyst **5** efficiently overcame the shortage of their interactions under the homogeneous catalysis conditions.

On the basis of this efficient aza–Michael addition/ATH cascade reaction, the **5**-catalyzed cascade reactions with a series of aryl-substituted enones and arylamines were further tested for the investigation of its general feasibility, as shown in Table 1. The results showed that all of the tested reactions could steadily proceed, producing the corresponding γ -secondary amino alcohols with high yields and enantioselectivities. Also, it was found that the yields and enantioselectivities were not significantly affected by the structures and electronic properties on the aromatic rings of Ar^2 group in the reaction of 1-phenylprop–2-enone and aromatic amines bearing electron-withdrawing and –donating substituents (Entries 4–12). However, in the case of the reactions of different aryl-substituted enone and aniline, the yields and enantioselectivities has an obvious changes, where the electron-withdrawing substituents on the aromatic rings of Ar^1 group had higher yields and lower *ee* values than those with electron-donating substituents (entries 13–20 versus entries 21–22).

3.2.2. Investigations of the factors affecting catalytic performance

To eliminate the affecting factors that the catalytic performance possibly comes from the contributions of the homogeneous MesRuTsDPEN via the noncovalent physical adsorption, one parallel experiment was performed, where this aza–Michael addition/ATH cascade reaction catalyzed by the physical mixture of **4** and homogeneous MesRuTsDPEN was carried out under the optimal reaction conditions. The result showed that the cascade reaction also yielded the corresponding (*S*)-1-phenyl-3-(phenylamino)propanol in 88% yield with 91% *ee* that was similar to that attained with the physically mixed *N,N*-dimethylprop–2-en–1-amine and homogeneous MesRuTsDPEN as dual catalysts (entry 3). However, the recycled catalyst **5** via a treatment of the Soxhlet extraction only produced tiny targeting products with the unconverted intermediate 1-phenyl-3-(phenylamino)propanone detected by the ^1H NMR analysis. A similar result was also observed via a parallel hot-filtrate experiment. In this case, this cascade reaction proceeded for 2 h at first. Subsequently, after a hot-filtration, the reaction was continued for a further 2.0 h. It was found that there was no appreciable change in either conversion or *ee* value of the targeting products. These findings disclosed that the contributions coming from the homogeneous MesRuTsDPEN via the noncovalent physical adsorption had been eliminated owing to the synthetic procedure via a strict Soxhlet extraction during the preparation process of catalyst **5**.

To demonstrate the catalytic nature of the aza–Michael addition/ATH cascade reaction, the time course in the reaction of 1-phenylprop–2-enone and aniline was also investigated, as shown in Fig. 5. Firstly, we found that the aza–Michael addition of 1-phenylprop–2-enone (**6a**) and aniline (**7a**) proceeds rapidly, and give intermediate 1-phenyl-3-(phenylamino)propanone (**A**) with 88% of maximum conversion within 10 min. In the next ten minutes, the conversion of **6a** is completed, the ATH of 1-phenyl-3-(phenylamino)propanone (**A**) occurred. Subsequently, the target product of (*S*)-1-phenyl-3-(phenylamino)propanol (**8a**) increased quickly from 20 min to 60 min that is concomitant with the gradual decrease of the intermediates **A**. Finally, the ATH of 1-phenyl-3-(phenylamino)propanone proceeds smoothly with a completed disappearance of **A** in 150 min, providing **8a** in 96% yield. Notably,

Table 1The aza–Michael addition/ATH enantioselective cascade reactions of aryl–substituted enones and amines.^a

Entry	Ar ¹ , Ar ² (8)	Time (h)	%Yield ^b	%ee ^c
1	Ph, Ph (8a)	2.5	96	96
2	Ph, Ph (8a)	12	92	96 ^d
3	Ph, Ph (8a)	12	86	91 ^e
4	Ph, 4–ClPh (8b)	4	91	96
5	Ph, 3–ClPh (8c)	3	92	95
6	Ph, 4–BrPh (8d)	3	91	97
7	Ph, 3–NO ₂ Ph (8e)	5	88	95
8	Ph, 4–CH ₃ Ph (8f)	4	93	96
9	Ph, 3,4–Me ₂ Ph (8g)	4	95	96
10	Ph, 3,5–Me ₂ Ph (8h)	4	92	95
11	Ph, 3–Cl–4–MePh (8i)	4	91	96
12	Ph, 3–CH ₃ OPh (8j)	3	90	96
13	4–FPh, Ph (8k)	2	91	93
14	3–FPh, Ph (8l)	2	95	93
15	2–FPh, Ph (8m)	2	90	90
16	4–ClPh, Ph (8n)	3	89	84
17	4–BrPh, Ph (8o)	3	87	94
18	4–IPh, Ph (8p)	3	91	93
19	4–NO ₂ Ph, Ph (8q)	4	92	80
20	4–CNPh, Ph (8r)	2	94	93
21	4–CH ₃ Ph, Ph (8s)	10	73	97
22	4–CH ₃ OPh, Ph (8t)	10	76	95

^a Reaction conditions: catalyst **5** (8.59 mg, 1.0 μmol of Ru based on ICP analysis, and 1.01 μmol of N based on TG analysis), enones (0.10 mmol), amines (0.11 mmol), HCOONa (1.0 mmol), 2.0 mL of ⁱPrOH/H₂O (v/v = 1:1), and reaction time (2.5–12 h).

^b Isolated yields.

^c The ee determined chiral HPLC analysis (see SI in Figs. S4, S6).

^d Data were obtained using physically mixed *N,N*-dimethylprop-2-en-1-amine and **3** as dual catalysts.

^e Data were obtained using physically mixed *N,N*-dimethylprop-2-en-1-amine and homogeneous MesRuTsDPEN as dual catalysts.

this reaction time course discloses a cascade process in this aza–Michael addition/ATH cascade reaction.

3.2.3. Extension of the aza–Michael addition/ATH cascade reaction

In addition to the general feasibility in the aza–Michael addition/ATH cascade reaction of enones and arylamines, this cascade reactions catalyzed by **5** could also be expanded to enones and

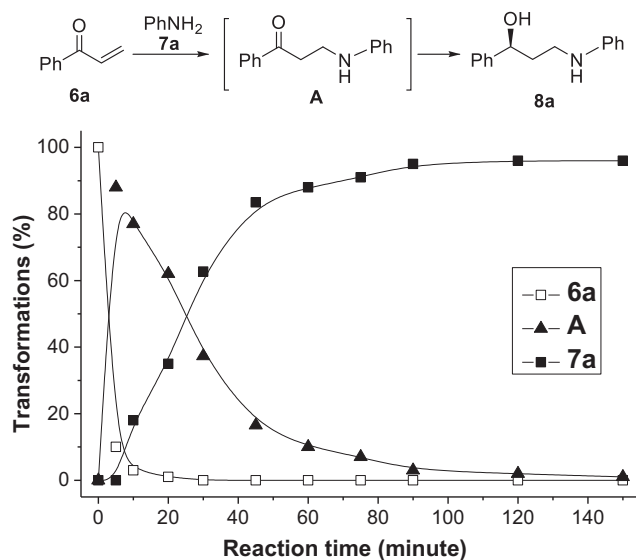
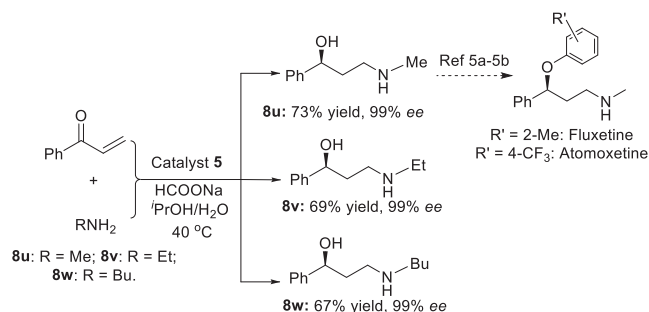


Fig. 5. Time course of the aza–Michael addition/ATH of 1–phenylprop-2–enone and aniline to (*S*)-1–phenyl-3–(phenylamino)propanol (reaction was performed with 1 equivalent of 1–phenylprop-2–enone, 1.1 equivalent of aniline, 1.0 mol% of catalyst **5**, 10.0 equivalent of HCOONa at 40 °C).

alkylamines since the targeting products were the important pharmaceutical intermediates for the preparation of optically pure antidepressants like Fluoxetine and Atomoxetine, as shown in **Scheme 3**. In this case, three representative alkylamines, methylamine, ethylamine, and butylamine, could steadily react with 1–phenylprop-2–enone in the **5**-catalyzed aza–Michael addition/ATH cascade reaction, providing chiral products in moderate yields with excellent enantioselectivities in environmentally friendly reaction conditions.

3.2.4. Catalyst's stability and recyclability

Besides general applications in the aza–Michael addition/ATH enantioselective cascade reaction, the heterobifunctional catalyst **5** also exhibited high recyclability. As shown in **Fig. 6**, catalyst **5** was recovered by a simple centrifugation and reused repeatedly, in six consecutive reactions for the aza–Michael addition/ATH of 1–phenylprop-2–enone and aniline, catalyst **5** still afforded 91%



Scheme 3. The **5**-catalyzed aza–Michael addition/ATH enantioselective cascade reactions of 1–phenylprop-2–enone and alkylamines.

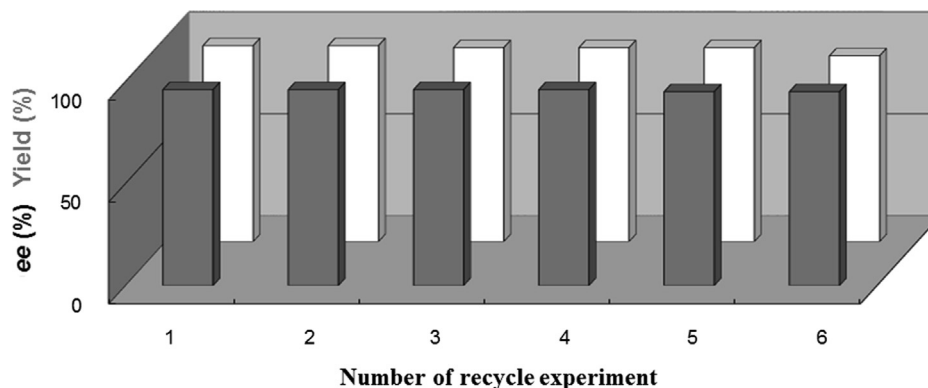


Fig. 6. Reusability of catalyst 5 using the cascade reduction of 1-phenylprop-2-enone and aniline.

yield and 95% *ee* (see SI in Table S1 and Fig. S5). The obviously decreased yield at the seventh recycle (82% yield with 91% *ee*) was possible due to the Ru-leaching of catalyst 5 during the recycling process, which could be proven by an inductively coupled plasma optical emission spectrometer (ICP-OES) analysis. It was found that Ru-loadings in catalyst 5 at the sixth and the seventh run were 11.29 mg/g and 10.42 mg/g, respectively, meaning the Ru-leachings at the seventh run were 12.52% relative to that of 5.21% at the sixth run. This finding indicated a large amount of Ru-loss in catalyst 5 was responsible for the decreased reactivity because of the presence of above 10% intermediate 1-phenyl-3-(phenylamino)propanone at the seventh run.

4. Conclusions

In conclusions, the integrated soluble polymer and mesoporous silica as a double-type support for the construction of heterobifunctional catalyst is developed by tethering tertiary amine-functionality in the outer polymer and anchoring chiral ruthenium/diamine-functionality within the inner silica. As presented in this study, this heterobifunctional catalyst performs an efficient aza-Michael addition/ATH one-pot enantioselective cascade reaction in an environmentally friendly medium. As we envisaged, the catalytically active site-isolated feature of catalyst, together with the tertiary amine-functionality for enhanced catalytic activity and the chiral ruthenium/diamine-functionality for maintainable enantioselective activity, ensure this cascade reaction to being converted into various chiral aryl-substituted γ -secondary amino alcohols with high yields and up to 99% enantioselectivity. In addition, the heterobifunctional catalyst can be recycled for the sixth runs, making it attractive in a practical preparation of γ -secondary amino alcohols.

Acknowledgments

We are grateful to the National Natural Science Foundation of China (21672149 and 21402120), and China postdoctoral science foundation (2018M642054) for financial support.

Appendix A. Supplementary material

Supplementary data to this article can be found online at <https://doi.org/10.1016/j.jcat.2019.07.005>.

References

[1] C.M.A. Parlett, M.A. Isaacs, S.K. Beaumont, L.M. Bingham, N.S. Hondow, K. Wilson, A.F. Lee, *Nat. Mater.* 15 (2016) 178–184.

[2] M.J. Climent, A. Corma, S. Iborra, *Chem. Rev.* 111 (2011) 1072–1133.
 [3] M.J. Climent, A. Corma, S. Iborra, M.J. Sabater, *ACS Catal.* 4 (2014) 870–891.
 [4] M.C.M. van Oers, F.P.J.T. Rutjes, J.C.M. Van Hest, *Curr. Opin. Biotechnol.* 28 (2014) 10–16.
 [5] S. Soled, *Science* 350 (2015) 1171–1172.
 [6] E.L. Margelefsky, R.K. Zeidan, M.E. Davis, *Chem. Soc. Rev.* 37 (2008) 1118–1126.
 [7] J.M. Thomas, R. Raja, *Acc. Chem. Res.* 41 (2008) 708–720.
 [8] C.G. Yu, J. He, *Chem. Commun.* 48 (2012) 4933–4940.
 [9] H.Q. Yang, L. Zhang, L. Zhong, Q.H. Yang, C. Li, *Angew. Chem. Int. Ed.* 46 (2007) 6861–6865.
 [10] C.E. Song, *Annu. Rep. Prog. Chem. Sect. C.* 101 (2005) 143–173.
 [11] M. Bartók, *Chem. Rev.* 110 (2010) 1663–1705.
 [12] S. Itsuno, *Polymeric Chiral Catalyst Design and Chiral Polymer Synthesis*, John Wiley & Sons, Inc., 2011.
 [13] M. Altava, I. Burguete, E. García-Verdugo, S.V. Luis, *Chem. Soc. Rev.* 47 (2018) 2722–2771.
 [14] Y.M. He, Y. Feng, Q.H. Fan, *Acc. Chem. Res.* 47 (2014) 2894–2906.
 [15] H.U. Blaser, E. Schmidt, *Asymmetric Catalysis on an Industrial Scale: Challenges, Approaches and Solutions*, Wiley-VCH, Weinheim, 2010.
 [16] J.N. Zhou, Q. Fang, Y.H. Hu, L.Y. Yang, F.F. Wu, L.J. Xie, J. Wu, S. Li, *Org. Biomol. Chem.* 12 (2014) 1009–1017.
 [17] A. Träff, R. Lihammar, J. Bäckvall, *J. Org. Chem.* 76 (2011) 3917–3921.
 [18] D.W. Robertson, J.H. Krushinski, R.W. Fuller, J.D. Leander, *J. Med. Chem.* 31 (1988) 1412–1417.
 [19] Y. Gao, K.B. Sharpless, *J. Org. Chem.* 53 (1988) 4081–4084.
 [20] H. Kakei, T. Nemoto, T. Ohshima, M. Shibasaki, *Angew. Chem. Int. Ed.* 43 (2004) 317–320.
 [21] Y. Fujima, M. Ikunaka, T. Inoue, J. Matsumoto, *Org. Process Res. Dev.* 10 (2006) 905–913.
 [22] S. Sakuraba, K. Achiwa, *Synlett.* 10 (1991) 689–690.
 [23] S. Sakuraba, K. Achiwa, *Chem. Pharm. Bull.* 43 (1995) 748–753.
 [24] D. Liu, W. Gao, C. Wang, X. Zhang, *Angew. Chem. Int. Ed.* 44 (2005) 1687–1689.
 [25] H. Geng, X. Zhang, M. Chang, L. Zhou, W. Wu, X. Zhang, *Adv. Synth. Catal.* 353 (2011) 3039–3043.
 [26] Q. Hu, Z. Zhang, Y. Liu, T. Imamoto, W. Zhang, *Angew. Chem. Int. Ed.* 54 (2015) 2260–2264.
 [27] J. Wang, Y. Wang, D. Liu, W. Zhang, *Adv. Synth. Catal.* 357 (2015) 3262–3272.
 [28] J. Wang, D. Liu, Y. Liu, W. Zhang, *Org. Biomol. Chem.* 11 (2013) 3855–3861.
 [29] L. Wu, R. Jin, L. Li, X. Hu, T. Cheng, G. Liu, *Org. Lett.* 19 (2017) 3047–3050.
 [30] L. Wu, Y. Li, J. Meng, R. Jin, J. Lin, G. Liu, *ChemPlusChem* 83 (2018) 861–867.
 [31] H. Liao, Y.J. Chou, Y. Wang, H. Zhang, T.Y. Cheng, G.H. Liu, *ChemCatChem* 9 (2017) 3197–3202.
 [32] J.Y. Xu, T.Y. Cheng, K. Zhang, Z.Y. Wang, G.H. Liu, *Chem. Commun.* 52 (2016) 6005–6008.
 [33] S. Hashiguchi, A. Fujii, J. Takehara, T. Ikariya, R. Noyori, *J. Am. Chem. Soc.* 117 (1995) 7562–7563.
 [34] T. Ohkuma, K. Tsutsumi, N. Utsumi, N. Arai, R. Noyori, K. Murata, *Org. Lett.* 9 (2007) 255–257.
 [35] P.N. Liu, P.M. Gu, F. Wang, Y.Q. Tu, *Org. Lett.* 6 (2004) 169–172.
 [36] A. Fujii, S. Hashiguchi, N. Uematsu, T. Ikariya, R. Noyori, *J. Am. Chem. Soc.* 118 (1996) 2521–2522.
 [37] M. Huang, L. Liu, S. Wang, H. Zhu, D. Wu, Z. Yu, S. Zhou, *Langmuir* 33 (2017) 519–526.
 [38] K. Zhang, L.L. Xu, J.G. Jiang, N. Calin, K.F. Lam, S.J. Zhang, H.H. Wu, G.D. Wu, B. Albela, L. Bonneviot, P. Wu, *J. Am. Chem. Soc.* 135 (2013) 2427–2430.
 [39] Z. Chen, W. Song, *Langmuir* 28 (2012) 13452–13458.
 [40] I. Mathakiya, V. Vangani, A.K. Rakshit, *J. Appl. Polym. Sci.* 69 (1998) 217–228.
 [41] D.E. Bergbreiter, P.L. Osburn, A. Wilson, E.M. Sink, *J. Am. Chem. Soc.* 122 (2000) 9058–9064.
 [42] O. Kröcher, O.A. Köppel, M. Fröba, A. Baiker, *J. Catal.* 178 (1998) 284–298.
 [43] X.J. Tang, Z.L. Yan, W.L. Chen, Y.R. Gao, S. Mao, Y.L. Zhang, Y.Q. Wang, *Tetrahedron: Lett.* 54 (2013) 2669–2673.
 [44] Y.M. He, Q.H. Fan, *ChemCatChem.* 7 (2015) 398–400.

- [45] X. Wu, X. Li, W. Hems, F. King, J. Xiao, *Org. Biomol. Chem.* 2 (2004) 1818–1821.
- [46] J.S. Wu, F. Wang, Y.P. Ma, X. Cui, L.F. Cun, J. Zhu, J.G. Deng, B.L. Yu, *Chem. Commun.* (2006) 1766–1768.
- [47] L. Wang, Q. Zhou, C. Qu, Q. Wang, L. Cun, J. Zhu, J. Deng, *Tetrahedron* 69 (2013) 6500–6506.
- [48] Z.S. Yang, F. Chen, Y.M. He, N.F. Yang, Q.H. Fan, *Catal. Sci. Technol.* 4 (2014) 2887–2890.
- [49] P.N. Liu, J.G. Deng, Y.Q. Tu, S.H. Wang, *Chem. Commun.* (2004) 2070–2071.